Unmanned Aerial Vehicle Guidance for an All-Aspect Approach to a Stationary Target

Group - **15**

Abel Viji George AE21B001
Abhigyan Roy AE21B002
Shreeya Padte AE21B056

Indian Institute of Technology
Madras

November 8, 2024

Introduction

This study focuses on developing a multiphase guidance algorithm for a UAV in the nonlinear engagement framework that enables an aerial vehicle to approach a stationary target from any direction. The challenges faced by the standard and two-phase Pure Proportional Navigation, mainly approach angle control are addressed, providing solutions that take into account the restrictions imposed by the seeker's field of view (FOV).
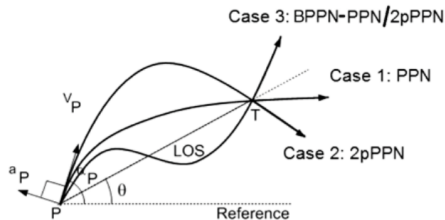

Figure 1: Possible terminal heading of UAV to a stationary target

Background

1. Importance of controlling approach angles for effective UAV operations.
   - Necessity of controlling terminal path angles includes requirements like efficient way-point navigation, achieving rendezvous, and other desired formations following a trajectory with sensing.
   - Controlling impact angle also becomes important in successful interception against stationary or slowly moving targets, such as aircraft carrier warships with efficient electronics countermeasures and a close-in weapon system.

2. Previous studies and their limitations.

Previous Studies on Impact Angle-Constrained Guidance Problem

Linearized Geometry-Based :

Work	Main Focus
1	Optimal-angle-based control guidance.
2	Sliding-mode-control-based guidance.
3	Zero-effort collision triangle was incorporated in a linear optimal guidance problem.

Limitation : The optimal-control-based approaches rely on linearization of the engagement problems and are sensitive to the time-to-go estimation error, while the sliding-mode-based approaches have limitations in dealing with scenarios with a relatively large initial heading error causing a positive initial range rate.

[1]Idan, M., Golan, O., and Guelman, M., "Optimal Planar Interception with Terminal Constraints," *Journal of Guidance, Control, and Dynamics*, Vol. 18, No. 6, Nov.–Dec. 1995, pp. 1273–1279. doi:10.2514/3.21541

[2]Kumar, S. R., and Ghose, D., "Three-Dimensional Impact Angle Guidance with Coupled Engagement Dynamics," *Journal of Aerospace Engineering*, Vol. 231, No. 4, April 2017, pp. 621–641. doi:10.1177/0954410016641442

[3]Cho, H., Ryoo, C. K., Tsourdos, A., and White, B., "Optimal Impact Angle Control Guidance Law Based on Linearization About Collision Triangle," *Journal of Guidance, Control, and Dynamics*, Vol. 37, No. 3, May–June 2014, pp. 958–964. doi:10.2514/1.62910

PN-Based :

Work	Main Focus
[4]	Time-varying biased pure PN.
[5], [6]	Two-stage planar pure PN (2pPPN) for stationary and lower-speed targets.
[7]	Composite PN-based guidance for higher-speed targets.

Limitation : They considered the impact-angle control for two-dimensional engagements and did not consider the FOV constraints.

[4]Kim, B. S., Lee, J. G., and Han, H. S., "Biased PNG Law for Impact with Angular Constraint," *IEEE Transactions on Aerospace and Electronic Systems*, Vol. 34, No. 1, Jan. 1998, pp. 277–288. doi:10.1109/7.640285

[5]Ratnoo, A., and Ghose, D., "Impact Angle Constrained Interception of Stationary Targets," *Journal of Guidance, Control, and Dynamics*, Vol. 31, No. 6, Nov.–Dec. 2008, pp. 1817–1822. doi:10.2514/1.37864

[6]Ratnoo, A., and Ghose, D., "Impact Angle Constrained Guidance Against Nonstationary Nonmaneuvering Targets," *Journal of Guidance, Control, and Dynamics*, Vol. 33, No. 1, Jan.–Feb. 2010, pp. 269–275. doi:10.2514/1.45026

[7]Ghosh, S., Ghose, D., and Raha, S., "Composite Guidance for Impact Angle Control Against Higher Speed Targets," *Journal of Guidance, Control, and Dynamics*, Vol. 39, No. 1, Jan. 2016, pp. 98–117. doi:10.2514/1.G001232
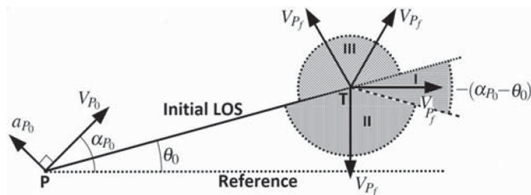
2-D Engagement Geometry

Figure 2: 2-D engagement geometry and UAV's terminal heading.

Engagement Equations for Stationary Target

$$\dot{R} = V_R = -V_P \cos(\alpha_P - \theta)$$

$$\dot{\theta} = \frac{V_\theta}{R} = -V_P \sin(\alpha_P - \theta)$$

$$\dot{\alpha_P} = \frac{a_P}{V_P}$$

The UAV's look angle is defined as $\mu = \alpha_P - \theta$

PPN

- The UAV's lateral acceleration is based on the pure PN (PPN) guidance law with the navigation gain N given by,

$$a_P = V_P \dot{\alpha_P} = N V_P \dot{\theta} \tag{1}$$

- The UAV's lateral acceleration is based on the pure PN (PPN) guidance law with the navigation gain N given by,

$$a_P = V_P \dot{\alpha_P} = N V_P \dot{\theta} \tag{1}$$

- Consider $\alpha_{P_0} \in [\theta_0, \theta_0 + \pi]$. In this case, from above equations, it follows that the achievable approach angle using the standard PPN guidance is given by

$$\alpha_{P_f} = \alpha_{P_0} + N(\theta_f - \theta_0)$$

- A collision course with a stationary target assumes $\alpha_{P_f} = \theta_f$

$$\alpha_{P_f} = \frac{(N\theta_0 - \alpha_{P_0})}{(N-1)}$$

PPN

- The UAV's lateral acceleration is based on the pure PN (PPN) guidance law with the navigation gain N given by,

$$a_P = V_P \dot{\alpha_P} = N V_P \dot{\theta} \qquad (1)$$

- Consider $\alpha_{P_0} \in [\theta_0, \theta_0 + \pi]$. In this case, from above equations, it follows that the achievable approach angle using the standard PPN guidance is given by

$$\alpha_{P_f} = \alpha_{P_0} + N(\theta_f - \theta_0)$$

- A collision course with a stationary target assumes $\alpha_{P_f} = \theta_f$

$$\alpha_{P_f} = \frac{(N\theta_0 - \alpha_{P_0})}{(N - 1)}$$

- For $N \geq 2$ (which is a condition for the bounded terminal lateral acceleration of the UAV), the achievable approach angle using PPN resides in the interval $\alpha_{P_f} \in [2\theta_0 - \alpha_{P_0}, \theta_0]$.

- However, $[2\theta_0 - \alpha_{P_0}, \theta_0) \subset [-\pi + \theta_0, \theta_0)$ which implies that using the standard PPN, a significant portion of the angular interval in the half-space $[-\pi + \theta_0, \theta_0)$ cannot be achieved. To expand the achievable approach angle set, a two-stage PPN guidance strategy (2pPPN) was introduced.

- However, $[2\theta_0 - \alpha_{P_0}, \theta_0) \subset [-\pi + \theta_0, \theta_0)$ which implies that using the standard PPN, a significant portion of the angular interval in the half-space $[-\pi + \theta_0, \theta_0)$ cannot be achieved. To expand the achievable approach angle set, a two-stage PPN guidance strategy (2pPPN) was introduced.

- For impact angles outside $[2\theta_0 - \alpha_{P_0}, \theta_0)$, an orientation guidance for the initial phase of missile flight was proposed. The purpose of orientation guidance is to take the missile from (α_{P_0}, θ_0) to $(\alpha_{P_{ORI_f}} = \theta_0, \theta_{ORI_f} = \theta_0 - \pi/2)$. Thus, the impact band covers $\alpha_{P_f} \in [-\pi + \theta_0, \theta_0]$.

- The gain for this phase is:

$$N_{ORI} = \frac{\theta_0 - \alpha_{P_0}}{\theta_0 - (\theta_0 - \pi/2)} = \frac{2}{\pi}|\alpha_{P_0} - \theta_0|$$

Theorem 1: Consider $\alpha_{P_0} > \theta_0$. A desired approach angle $\alpha_{P_f}^d$ $\in [2\theta_0 - \alpha_{P_0}, \theta_0)$ could be attained by PPN with $N = \frac{\alpha_{P_f}^d - \alpha_P}{\alpha_{P_f}^d - \theta} \geq 2$,

whereas $\alpha_{P_f}^d \in [-\pi + \theta_0, 2\theta_0 - \alpha_{P_0})$ could be achieved by 2pPPN with

$$
N = \begin{cases} \frac{2}{\pi}(\alpha_{P_0} - \theta_0); & \text{if } \frac{\alpha_{P_f}^d - \alpha_P}{\alpha_{P_f}^d - \theta} < 2 \\ \frac{\alpha_{P_f}^d - \alpha_P}{\alpha_{P_f}^d - \theta}; & \text{if } \frac{\alpha_{P_f}^d - \alpha_P}{\alpha_{P_f}^d - \theta} \geq 2 \end{cases}
$$

Examples of trajectories using PPN for $\alpha_{P_f}^d = -\pi/6$ and 2pPPN for $\alpha_{P_f}^d = -5\pi/6$ are presented, with and without the look-angle constraint.

2pPPN

Observation 1: Consider $\alpha_{P_0} < \theta_0$. A desired approach angle $\alpha_{P_f}^d$ $\in (\theta_0, 2\theta_0 - \alpha_{P_0}]$ could be attained by PPN with $N = \frac{\alpha_{P_f}^d - \alpha_P}{\alpha_{P_f}^d - \theta} \geq 2$, whereas $\alpha_{P_f}^d \in (2\theta_0 - \alpha_{P_0}, -\pi + \theta_0]$ could be achieved by 2pPPN with

$$N = \begin{cases} \frac{2}{\pi}|(\alpha_{P_0} - \theta_0)| & \text{if } \frac{\alpha_{P_f}^d - \alpha_P}{\alpha_{P_f}^d - \theta} < 2 \\ \frac{\alpha_{P_f}^d - \alpha_P}{\alpha_{P_f}^d - \theta} & \text{if } \frac{\alpha_{P_f}^d - \alpha_P}{\alpha_{P_f}^d - \theta} \geq 2 \end{cases}$$

Observation 2: If $\alpha_{P_0} = \theta_0$ or $\alpha_{P_0} = -\pi + \theta_0$, then before applying Theorem 1 and Observation 1, an engagement geometry (α_P, θ) needs to be attained outside the collision course or inverse collision course by using a finite adjustment pulse bias B_{adj} satisfying

$$sgn(B_{adj}) = \begin{cases} -sgn(\alpha_{P_f}^d - \theta_0) & \text{if } \alpha_{P_0} = \theta_0 \\ sgn(\alpha_{P_f}^d - \theta_0) & \text{if } \alpha_{P_0} = -\pi + \theta_0 \end{cases}$$

Three-Phase Composite Guidance

- To overcome the limit of angular spectrum for achievable terminal angles, the reversal of the LOS rate is found to be crucial. This can be facilitated by adding a finite bias profile "$Bsgn(\dot{\theta}_0)$" to the PPN guidance command for a certain time interval (Biased PPN or BPPN).

Three-Phase Composite Guidance

- To overcome the limit of angular spectrum for achievable terminal angles, the reversal of the LOS rate is found to be crucial. This can be facilitated by adding a finite bias profile "$Bsgn(\dot{\theta}_0)$" to the PPN guidance command for a certain time interval (Biased PPN or BPPN).

- For PPN, $\dot{\mu} = (N-1)\dot{\theta} = -(N-1)V_P sin(\mu)/R$. Hence, depending on the initial value of μ, it monotonically increases or decreases to 0, which implies that $\dot{\theta}$ is sign-preserving.
  Proof:
  - $a_P = NV_P\dot{\theta} + Bsgn(\dot{\theta}_0)$
  - $\dot{\mu} = -(N-1)V_P sin\mu/R + (B/V_P)sgn(\dot{\theta}_0)$.
  - From eqn of $\dot{\theta}$, $\dot{\theta}_0$ decreases (increases) if $\mu_0 > 0$ ($\mu_0 < 0$). Hence, $\frac{d|\mu|}{dt} < -(N-1)V_P|sin\mu|/R$. So, $|\mu|$ goes to zero faster than R and hence, LOS rate changes sign.

αCIG Law and Algorithm:

Assume that the initial conditions are such that the desired approach angle is not attainable by the PPN or the 2pPPN guidance laws alone. In that case,

1. In phase-1, use BPPN guidance, $a_P^{\alpha CIG} = NV_P\dot{\theta} + Bsgn(\dot{\theta_0})$ with $N = 2$ and $B > 0$ for an interval from $t = 0$ to $t = t_2$. t_2 is the time at which $\dot{\theta}$ changes sign. $\theta(t_2) = \theta_2$, $\alpha_P(t_2) = \alpha_{P_2}$.

αCIG Law and Algorithm:

Assume that the initial conditions are such that the desired approach angle is not attainable by the PPN or the 2pPPN guidance laws alone. In that case,

1. In phase-1, use BPPN guidance, $a_P^{\alpha CIG} = NV_P\dot{\theta} + Bsgn(\dot{\theta}_0)$ with $N = 2$ and $B > 0$ for an interval from $t = 0$ to $t = t_2$. t_2 is the time at which $\dot{\theta}$ changes sign. $\theta(t_2) = \theta_2$, $\alpha_P(t_2) = \alpha_{P_2}$.

2. In phase-2, use BPPN guidance again with $N < 1$ and $B > 0$ till a time $t = t_3$. $\theta(t_3) = \theta_3$ such that $\theta_3 \in [\theta_2, \theta_0]$ or $\theta_3 \in [\theta_0, \theta_2]$ and $\alpha_{Pf}^d \in [\theta_0, \theta_3 + \pi]$ or $\alpha_{Pf}^d \in [-\pi + \theta_3, \theta_0]$ for $\alpha_{P0} > \theta_0$ or $\alpha_{P0} < \theta_0$, respectively.

αCIG Law and Algorithm:

Assume that the initial conditions are such that the desired approach angle is not attainable by the PPN or the 2pPPN guidance laws alone. In that case,

1. In phase-1, use BPPN guidance, $a_P^{\alpha CIG} = NV_P\dot{\theta} + Bsgn(\dot{\theta}_0)$ with $N = 2$ and $B > 0$ for an interval from $t = 0$ to $t = t_2$. t_2 is the time at which $\dot{\theta}$ changes sign. $\theta(t_2) = \theta_2$, $\alpha_P(t_2) = \alpha_{P_2}$.

2. In phase-2, use BPPN guidance again with $N < 1$ and $B > 0$ till a time $t = t_3$. $\theta(t_3) = \theta_3$ such that $\theta_3 \in [\theta_2, \theta_0]$ or $\theta_3 \in [\theta_0, \theta_2]$ and $\alpha_{Pf}^d \in [\theta_0, \theta_3 + \pi]$ or $\alpha_{Pf}^d \in [-\pi + \theta_3, \theta_0]$ for $\alpha_{P0} > \theta_0$ or $\alpha_{P0} < \theta_0$, respectively.

3. In phase-3, use 2pPPN guidance law $a_{\alpha_{CIG}} = NV_P\dot{\theta}$ with navigation gain N defined as $N = \frac{2}{\pi}|\alpha_{P3} - \theta_3|$ as long as $(\alpha_{Pf}^d - \alpha_P)/(\alpha_{Pf}^d - \theta) < 2$; otherwise, set $N = (\alpha_{Pf}^d - \alpha_P)/(\alpha_{Pf}^d - \theta)$. This applies if α_{Pf}^d lies within $[2\theta_3 - \alpha_{P3}, \pi + \theta_3]$ or $[-\pi + \theta_3, 2\theta_3 - \alpha_{P3}]$ for initial conditions $\alpha_{P0} > \theta_0$ or $\alpha_{P0} < \theta_0$, respectively.

Similar to αCIG Law, but here we have the added constraint of the look angle, which adds a few more additional steps. Given α_{P_0} and $\alpha_{P_f}^d$,

1. Use BPPN, $a_P^{\mu\alpha_{CIG}} = NV_P\dot{\theta} + B\text{sgn}(\dot{\theta}_0)$ with $N = 2$ and B finite and positive until time t_1, at which $|\mu|$ becomes just less than μ_s if $|\mu_0| = |\alpha_{P_0} - \theta_0| \in [\mu_s, \pi]$. Let $\alpha_P(t_1) = \alpha_{P_1}$ and $\theta(t_1) = \theta_1$. Else, if $|\mu_0| \in [0, \mu_s]$, then $t_1 = t_0$, $\alpha_P(t_1) = \alpha_{P_1} = \alpha_{P_0}$, and $\theta(t_1) = \theta_1 = \theta_0$.

Similar to αCIG Law, but here we have the added constraint of the look angle, which adds a few more additional steps. Given α_{P_0} and $\alpha_{P_f}^d$,

1. Use BPPN, $a_P^{\mu\alpha CIG} = NV_P\dot{\theta} + B\text{sgn}(\dot{\theta_0})$ with $N = 2$ and B finite and positive until time t_1, at which $|\mu|$ becomes just less than μ_s if $|\mu_0| = |\alpha_{P_0} - \theta_0| \in [\mu_s, \pi]$. Let $\alpha_P(t_1) = \alpha_{P_1}$ and $\theta(t_1) = \theta_1$. Else, if $|\mu_0| \in [0, \mu_s]$, then $t_1 = t_0$, $\alpha_P(t_1) = \alpha_{P_1} = \alpha_{P_0}$, and $\theta(t_1) = \theta_1 = \theta_0$.

2. In phase-1, use BPPN guidance, $a_P^{\mu\alpha CIG} = NV_P\dot{\theta} + B\text{sgn}(\dot{\theta_0})$ with $N = 2$ and $B > 0$ for an interval from $t = 0$ to $t = t_2$. t_2 is the time at which $\dot{\theta}$ changes sign. $\theta(t_2) = \theta_2$, $\alpha_P(t_2) = \alpha_{P_2}$.

③ In the phase-2, use the look-angle-constrained bias-shaped BPPN guidance $a_P^{\mu\alpha_{CIG}} = NV_P\dot{\theta} + B\text{sgn}(\theta_1)$ with $N < 1$ and $B > 0$ at time $t \geq t_2$ as long as, for $\alpha_{P_1} > \theta_1$, $\theta < \alpha_{P_f}^d$ and

$$(N - 1)V_P(\theta - \theta_2) < \int_{t_2}^t B\,dt < (N - 1)V_P(\theta - \theta_2) + V_P\mu_s;$$

or for $\alpha_{P1} < \theta_1$, $\theta > \alpha_{P_f}^d$ and

$$(N - 1)V_P(\theta_2 - \theta) < \int_{t_2}^t B\,dt < (N - 1)V_P(\theta_2 - \theta) + V_P\mu_s.$$

upto a time $\hat{t}$. $\theta(\hat{t}) = \hat{\theta}$ and $\alpha_P(\hat{t}) = \hat{\alpha_P}$.

$\mu\alpha$CIG Law and Algorithm:

3. In the phase-2, use the look-angle-constrained bias-shaped BPPN guidance $a_P^{\mu\alpha CIG} = NV_P\dot{\theta} + B\text{sgn}(\theta_1)$ with $N < 1$ and $B > 0$ at time $t \geq t_2$ as long as, for $\alpha_{P_1} > \theta_1$, $\theta < \alpha_{P_f}^d$ and

$$(N-1)V_P(\theta - \theta_2) < \int_{t_2}^t B\, dt < (N-1)V_P(\theta - \theta_2) + V_P\mu_s;$$

or for $\alpha_{P1} < \theta_1$, $\theta > \alpha_{P_f}^d$ and

$$(N-1)V_P(\theta_2 - \theta) < \int_{t_2}^t B\, dt < (N-1)V_P(\theta_2 - \theta) + V_P\mu_s.$$

upto a time $\hat{t}$. $\theta(\hat{t}) = \hat{\theta}$ and $\alpha_P(\hat{t}) = \hat{\alpha_P}$.

- If $\alpha_{P_f}^d \in (\hat{\theta}, \hat{\theta} + \pi]$ or $\alpha_{P_f}^d \in [-\pi + \hat{\theta}, \hat{\theta})$ for $\alpha_{P_1} > \theta_1$ or $\alpha_{P_1} < \theta_1$, respectively, then $t_3 = \hat{t}$, $\alpha_{P_3} = \hat{\alpha_P}$, and $\theta_3 = \hat{\theta}$. Begin the third phase as specified in Step 4.

- Continue with the look-angle-constrained BPPN guidance $a_P^{\mu\alpha CIG} = NV_P\dot{\theta} + B\text{sgn}(\theta_1)$ with $N = 1$ and $B = 0$ until $\theta = \theta_3$ at some time t_3 such that $\alpha_{P_f}^d \in (\theta_3, \theta_3 + \pi]$ or $\alpha_{P_f}^d \in [-\pi + \theta_3, \theta_3)$, if $\hat{\theta} < -\pi + \alpha_{P_f}^d$ or $\hat{\theta} > \pi + \alpha_{P_f}^d$ for $\alpha_{P_1} > \theta_1$ or $\alpha_{P_1} < \theta_1$, respectively, let $\alpha_P(t_3) = \alpha_{P_3}$. At time $t = t_3$, start the third phase as in Step 4.

④ In phase-3,

- Use PPN guidance with $a_P^{\mu\alpha CIG} = NV_P\dot\theta$, where
$N = (\alpha_{P_f}^d - \alpha_{P_3})/(\alpha_{P_f}^d - \theta_3)$, if $\alpha_{P_f}^d \in (\theta_3, 2\theta_3 - \alpha_{P_3}]$ or
$\alpha_{P_f}^d \in [2\theta_3 - \alpha_{P_3}, \theta_3)$ for $\alpha_{P_1} > \theta_1$ or $\alpha_{P_1} < \theta_1$, respectively.

- Use 2pPPN guidance law $a_P^{\mu\alpha CIG}$ with navigation gain N defined as
$N = \frac{2}{\pi}|\alpha_{P3} - \theta_3|$ as long as $(\alpha_{Pf}^d - \alpha_P)/(\alpha_{Pf}^d - \theta) < 2$; otherwise, set
$N = (\alpha_{Pf}^d - \alpha_P)/(\alpha_{Pf}^d - \theta)$. This applies if α_{Pf}^d lies within
$(2\theta_3 - \alpha_{P3}, \pi + \theta_3]$ or $[-\pi + \theta_3, 2\theta_3 - \alpha_{P3})$ for initial conditions
$\alpha_{P_1} > \theta_1$ or $\alpha_{P_1} < \theta_1$, respectively.

Simulation Setup and Results

- All the results presented were simulated in MATLAB.
- The target is stationary and in line with the pursuer initially ($\theta_0 = 0$)
- The initial angle of the pursuer (α_{P0}) is 45° for 2pPPN and 135° for the Three-phase Composite guidance, αCIG and $\mu\alpha$CIG laws.

$\alpha_{P_f}^d$, rad	Guidance	First phase			Second phase			
		N	B	t_2, s	N	B	t_3, s	θ_3, rad
0	αCIG	2	$V_P\|\alpha_P\|/5$	27.09	-2	$V_P\|\alpha_P\|/10$	37.82	-0.071
0	$\mu\alpha$CIG	2	$V_P\|\alpha_P\|/5$	27.29	-2	$V_P\|\alpha_P\|/10$	32.57	-0.213
$\pi/3$	αCIG	2	$V_P\|\alpha_P\|/5$	27.09	-2	$V_P\|\alpha_P\|/10$	37.82	-0.071
$\pi/3$	$\mu\alpha$CIG	2	$V_P\|\alpha_P\|/5$	27.29	-2	$V_P\|\alpha_P\|/10$	32.57	-0.213
$5\pi/6$	αCIG	2	$V_P\|\alpha_P\|/5$	27.09	-2	$V_P\|\alpha_P\|/10$	37.82	-0.071
$5\pi/6$	$\mu\alpha$CIG	2	$V_P\|\alpha_P\|/5$	27.29	-2	$V_P\|\alpha_P\|/10$	32.57	-0.213

Trajectory Analysis and Look Angle for Two Phase PPN (paper)
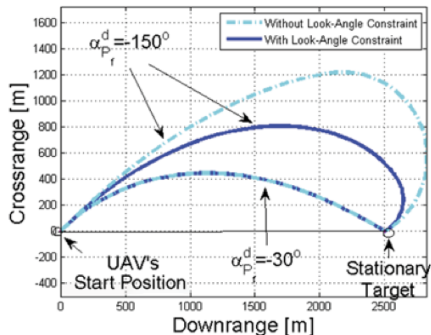
Figure 3: UAV's trajectory for PPN and 2pPPN for $\alpha_{p_f}^d = -30°$ and $-150°$.
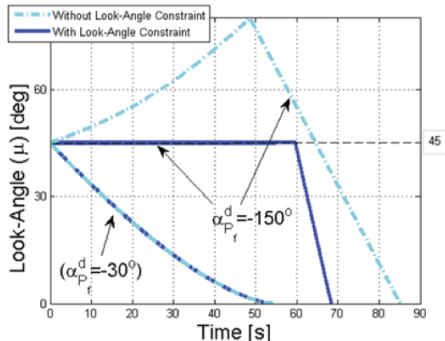
Figure 4: Variation of Look-Angle with time.
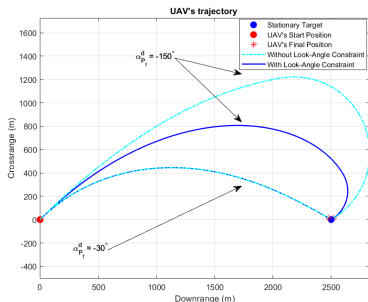
Figure 5: UAV's trajectory for PPN and 2pPPN for $\alpha_{p_f}^d = -30°$ and $-150°$.
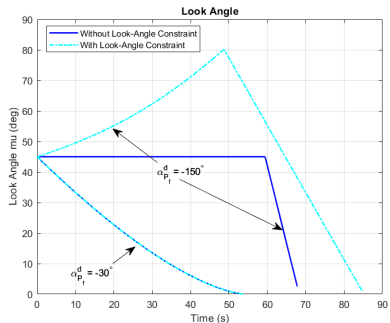
Figure 6: Variation of Look-Angle with time.

Example of three-phase composite guidance
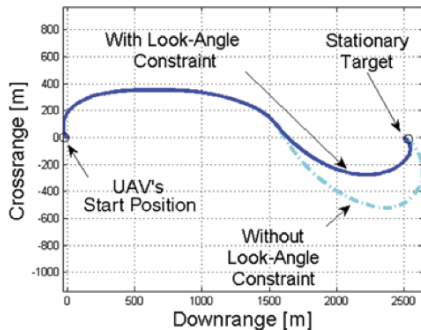
Figure 7: UAV's trajectory for $\alpha_{p_f}^d = 150°$. (Paper)
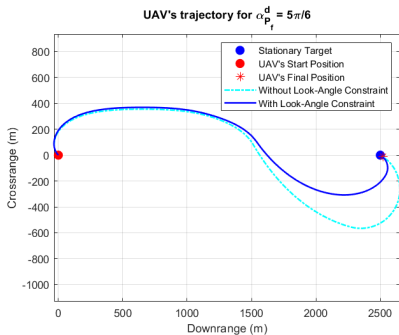
Figure 8: UAV's trajectory for $\alpha_{p_f}^d = 150°$. (Code)

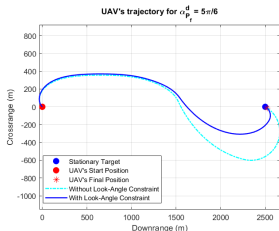# 2-D engagement with $\alpha_{P_f}^d = 0$ (paper)
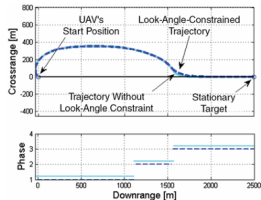
Figure 9: UAV's Trajectory
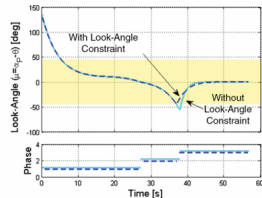
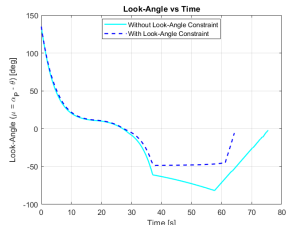
Figure 10: Look-Angle over Time
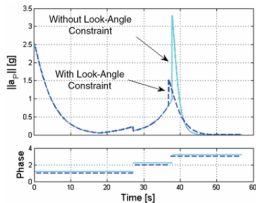
Figure 11: Lateral Acceleration Requirement
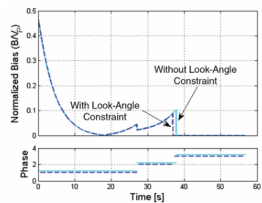
Figure 12: Bias Variation over Time

2-D engagement with $\alpha_{P_f}^d = 0$ (code)
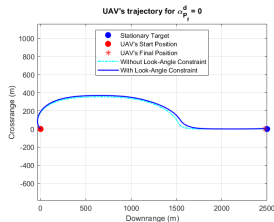
Figure 13: UAV's Trajectory
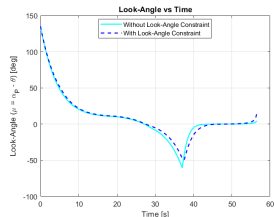
Figure 14: Look-Angle over Time
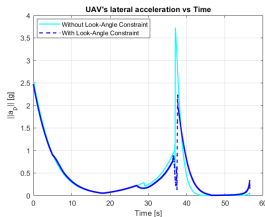
Figure 15: Lateral Acceleration Requirement
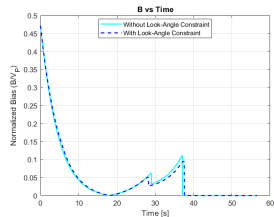
Figure 16: Bias Variation over Time

2-D engagement with $\alpha_{P_f}^d = \pi/3$ (paper)
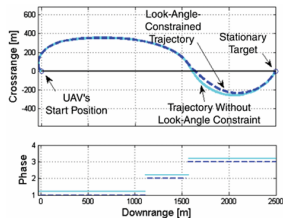
Figure 17: UAV's Trajectory
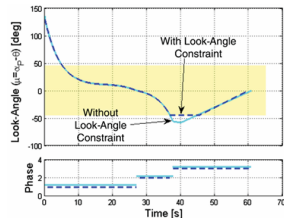
Figure 18: Look-Angle over Time
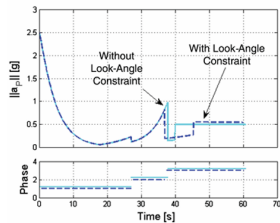

Figure 19: Lateral Acceleration Requirement
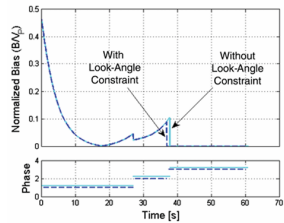

Figure 20: Bias Variation over Time
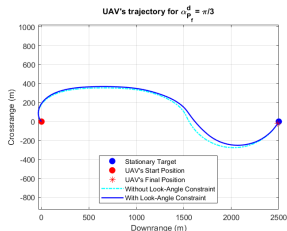
Figure 21: UAV's Trajectory
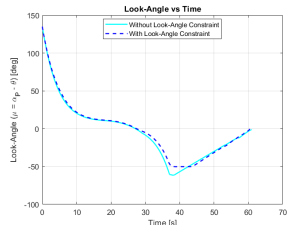
Figure 22: Look-Angle over Time
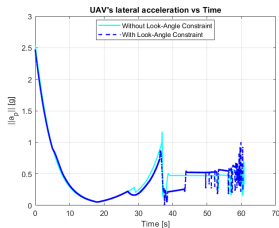
Figure 23: Lateral Acceleration Requirement
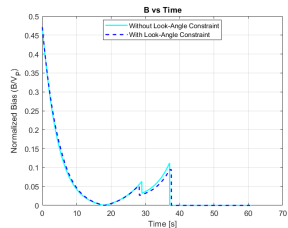
Figure 24: Bias Variation over Time
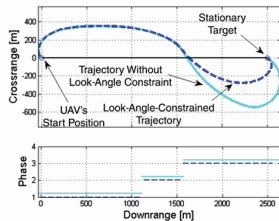
Figure 25: UAV's Trajectory
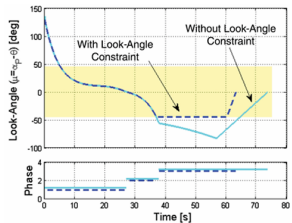
Figure 26: Look-Angle over Time
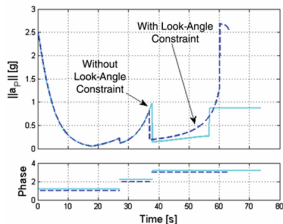
Figure 27: Lateral Acceleration Requirement
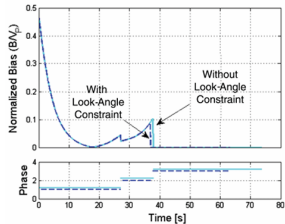
Figure 28: Bias Variation over Time

Figure 29: UAV's Trajectory

Figure 30: Look-Angle over Time
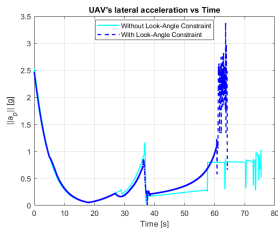
Figure 31: Lateral Acceleration Requirement
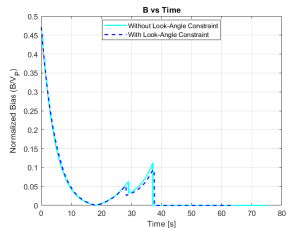
Figure 32: Bias Variation over Time

αCIG and $\mu\alpha$CIG with varied constant Bias profiles (paper)
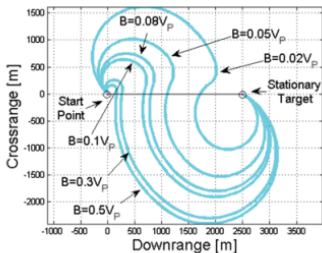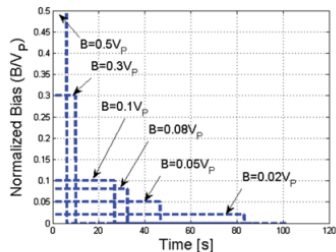

a) αCIG trajectories
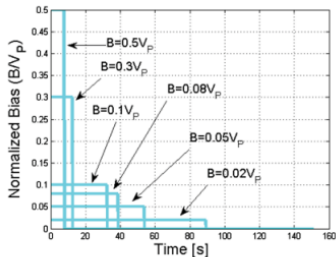
b) αCIG bias profiles
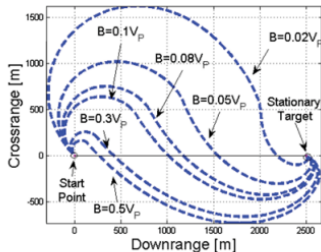
c) $\mu\alpha$CIG trajectories

d) $\mu\alpha$CIG bias profiles

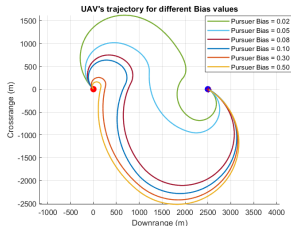# αCIG and $\mu\alpha$CIG with varied constant Bias profiles (code)

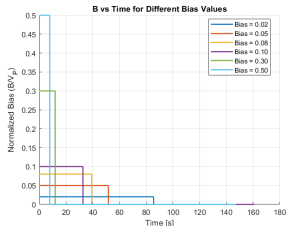Figure 33: αCIG Trajectories
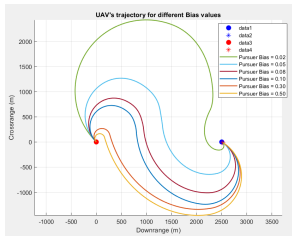

Figure 34: αCIG Bias Profiles

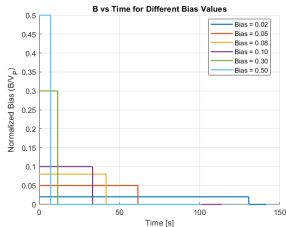Figure 35: $\mu\alpha$CIG Trajectories

Figure 36: $\mu\alpha$CIG Bias Profiles

Summary

- As seen, implementing the $\mu\alpha$CIG Law , a full circle approach angle set $[-\pi, \pi)$ can be achieved while satisfying the FOV constraint which gives a bias-shaped BPPN guidance .
- Implications for UAV operations in real-world scenarios and Potential applications of developed guidance strategies.
  - Precision strikes and surveillance missions
  - Infrastructure Inspection
  - Search and Rescue Missions

Future Work

Extensions

- Furthering the work in this paper, we can implement a modified law for non-stationary targets, starting with constant velocity targets and extending to maneuvering targets.

- Also, we can add environmental conditions like wind velocity or turbulence like drag as variables in the engagement equations of the UAV.

The paper also has implemented the same for 3D engagements and SITL simulations, which we have not discussed due to time constraints.